SOME CONSIDERATIONS ON SOUND SYNTHESIS OF PIANO HAMMER/STRING COLLISION

PACS Reference: 43.75.Mn

Christophe Vergez,[1] René Caussé,[2] Eric Humbert,[2] et Olivier de Lajudie[2]

[1]LMA, CNRS, 31 Chemin Joseph Aiguier, 13402 Cedex 20 Marseille, France, email: vergez@lma.cnrs-mrs.fr
[2]IRCAM, Centre Pompidou/CNRS, 1 pl. Igor Stravinsky, 75004 Paris, France, email: causse,humbert@ircam.fr

ABSTRACT

The contact between the piano hammer and the string is considered within a sound synthesis framework. Particular attention is paid to the model of the felt around the hammer head.

I. INTRODUCTION

This work has been done in the framework of sound synthesis. For approximately ten years, physical modelling has been used for sound synthesis aimed at musical applications. Among other ways of producing sound with physical models, collision models between objects have been widely used by musicians in their music. This is probably due to the rather intuitive way of controlling the corresponding models. Indeed, no matter how objects are being struck in the simulation, sound is produced. On the other hand, this is far from being true for models of self-sustained instruments for which auto-oscillation results from the precise adjustment of the control parameters. However, a common feature of self-sustained and percussive instruments is that most of the time, very simple models are able to produce satisfying results from a perceptive point of view. Thus, simple models of percussive instruments have been used both in a musical context ([1] for example) and in psychoacoustics ([2]).

Practically, a large range of percussive sounds can be generated by a simple striking model based on elastic collision principle. Such a model has been implemented in the *Modalys* software (physical modelling environment) developed at Ircam for more than ten years (see [3] for the first implementation).

The case of the piano is particularly interesting. In fact, a lack of realism can often be noted in synthesized sounds. A first reason is probably that real piano sounds are very familiar to listeners. Another reason could be that reducing a complex instrument like the piano (including two or three strings by note, a bridge on a constraint soundboard, complex radiating patterns ...) to an impact between the hammer and one (or even two or three) non-radiating string(s) is a crude approximation. However, while a plucked string is not a less crude approximation of the guitar, synthesis results in a more realistic sound. More disturbingly, synthesis of struck strings often do sound like plucked strings !

This work has been carried out, as previously said, in the framework of sound synthesis and is motivated by feedback of musicians and our own experience in synthesizing piano sounds using physical models. A single non-radiating string fixed at both ends is first considered within *Modalys* environment. The most striking artefacts are summarized in section II.2. Some of them are obviously due to the absence of coupling with other strings via the bridge and the soundboard, which can easily be checked by including the missing elements in *Modalys* simulations. On the other hand we concentrate in this article on the hammer/string collision. The lumped elastic collision model (noted LECM in the following) detailed in section II.3, turns out to be responsible for other artefacts at contact time between the hammer and the string (see section II.4). It is then highlighted how simulation results are improved including a massless visco-elastic interface layer. This interface layer corresponds to the felt surrounding the wood head of real piano hammers. Its visco-elastic properties are modelled using Stulov approach ([4]).

II. ANALYSIS OF SIMULATION RESULTS USING THE LUMPED ELASTIC COLLISION MODEL

II.1. Sound Synthesis Framework

Sound synthesis results analysed in this section have been produced using *Modalys* software. *Modalys* is a sound synthesis software developed at Ircam for research and musical applications. Within *Modalys*, models of musical instruments are made of mechanical/acoustical interactions (blow, strike, pluck, bow ...) between resonating components (strings, tubes, plates, membranes, bridges, soundboard,...). The dynamics of each resonating component are calculated within its own modal basis. Modal data include natural frequencies, damping factors and deflection shapes.

II.2. Typical Artefacts Often Encountered

Let us now consider typical artefacts produced by a basic piano model made by a hammer striking a single unidimensional string fixed at its both ends.

We do not focus here on artefacts which are obviously due to the crude representation of the resonating part. For example, it is well known that the typical double decay phenomenon cannot be obtained with such a simple system ([5]). Moreover spectral differences between the sound synthesized and a real piano sound can also be explained by the absence of a soundboard ([6]).

We concentrate in the following on two major artefacts caused (as shown in section II.4) by the LECM :

- There is a click at contact time during the synthesis when listening at the striking point.

- More disturbingly, simulation results often sound as a plucked string would do.

Note that while we have experienced that the sound quality (in terms of resemblance to natural sounds) of the synthesis is largely improved by taking into account two or three strings and their coupling through the bridge to the soundboard, the two artefacts mentionned above remain audible. In the next section, the (very general) LECM used in *Modalys* is described, and an explanation of the artefacts mentioned above is proposed.

II.3. Lumped Elastic Collision Model (LECM)

In the collision model considered here, only one point of each object is concerned with the collision. That's why it is called a lumped model.

Since the contact occurs between a single point of each structure, the problem can be described without any loss of generality by the collision between two mass/spring systems (i.e. single-mode systems).

Before any contact, the hammer and the string are governed by equations (1a) and (1b) respectively plus initial conditions:

$$\begin{cases} \sum \overrightarrow{F_h} = m_h \overrightarrow{a_h} & (1a) \\ \sum \overrightarrow{F_s} = m_s \overrightarrow{a_s} & (1b) \end{cases} \quad (1)$$

where $''h''$ stands for "hammer" and $''s''$ for "string", $\overrightarrow{F}$ denotes the forces applied on an object, m is the mass of the object and $\overrightarrow{a}$ its acceleration. Equations (1a) and (1b) are uncoupled until collision.

The collision is supposed to be elastic, which means non dissipative. When contact occurs (at time $t = t_c$), momentum and energy are conserved.

Momentum conservation, once projected on an axis perpendicular to the string direction (the hammer and the string are supposed to strike perpendicularly) leads to:

$$m_h v_h^- + m_s v_s^- = m_h v_h^+ + m_s v_s^+ \quad (2)$$

where $''-''$ and $''+''$ denote the time just before and after the contact, and v is the velocity of the object considered.

Since trajectory of the contact point is continuous, energy conservation is equivalent to kinetic energy conservation:

$$m_h \left(v_h^-\right)^2 + m_s \left(v_s^-\right)^2 = m_h \left(v_h^+\right)^2 + m_s \left(v_s^+\right)^2 \quad (3)$$

Solving equations (2) and (3) allows us to express velocities just after contact according to velocities just

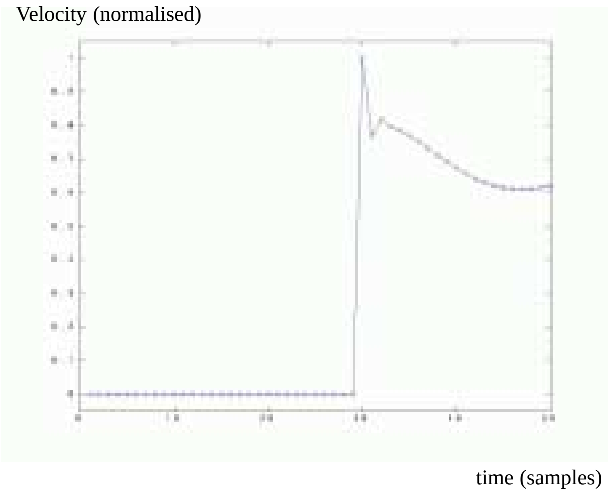

Figure 1: Normalised velocity v_s of the struck point in a string, with a discontinuity at contact time. The simulation uses the collision model described in section II.3.

before contact through the following well-known equation:

$$\begin{pmatrix} v_h^+ \\ \\ v_s^+ \end{pmatrix} = \begin{bmatrix} \dfrac{m_h - m_s}{m_h + m_s} & \dfrac{2m_s}{m_h + m_s} \\ \\ \dfrac{2m_h}{m_h + m_s} & -\dfrac{m_h - m_s}{m_h + m_s} \end{bmatrix} \begin{pmatrix} v_h^- \\ \\ v_s^- \end{pmatrix} \quad (4)$$

From equation (4), it can be checked that at time $t = t_c$, the velocity of both points involved in the collision undergoes a jump:

$$\begin{cases} [\![v_h]\!]_{t_c} \triangleq v_h^+ - v_h^- = -\dfrac{2m_s}{m_h + m_s}\left(v_h^- - v_s^-\right) & (5a) \\ [\![v_s]\!]_{t_c} \triangleq v_s^+ - v_s^- = \dfrac{2m_h}{m_h + m_s}\left(v_h^- - v_s^-\right) & (5b) \end{cases} \quad (5)$$

This jump of velocity corresponds to an impulsional force at $t = t_c$ ([7]). Thus, the jump undergone by velocities v_h and v_s is non zero except when hammer and string velocities are the same just before collision ($v_h^- = v_s^-$).

In practice, in the algorithm used by *Modalys*, the dynamics of each object at next time step is calculated with an Euler scheme to solve system (1). Since the unknown variables in the solving process are velocities, knowing v_h^+ and v_s^+ is enough to calculate the velocities one time step after the contact.

II.4. Discussion

II.4.1. Clicks at contact time

According to section II.3, it is easy to understand why the velocity of the struck point in the string is discontinuous at contact time. This is simply due to an instantaneous momentum transfer at constant energy. A click is heard, especially when the signal listened is the velocity, as it is the case by default in *Modalys* . On figure 1, velocity v_s of the contact point in the string is plotted using a more complete modal decomposition of the string (fourty modes in this example). The string, which corresponds to the note $A3$ ($220Hz$), is at rest before collision. The hammer (modeled as a 1-mode system) is launched with an initial velocity $v_0 = 1\text{m.s}^{-1}$, starting from an initial position under the string. Therefore, it is only submitted to gravity. The string is struck at one eighth of its length.

II.4.2. Resemblance between plucked and struck strings

We have experienced that with the collision model described in II.3, impulsional contacts are likely to occur in simulations. While this is yet to be proved, it can be supposed that this is responsible for the resemblance with plucked strings. Indeed, the duration of contact between the hammer and the string of a real piano is far from being reduced to a single instant t_c. This has been discussed by many authors ([8] for example).

II.4.3. Need for another model of sound synthesis

We study in the next section a way of coping with the two artefacts mentioned in this section. Our proceedure is therefore mainly dictated by the desire of eliminating clicks at contact time and to simulate more realistic durations of contact.

III. INTRODUCING VISCO-ELASTIC INTERFACE BETWEEN THE HAMMER HEAD AND THE STRING

III.1. Refinement Of The Model

According to equation (4), a simple way of preventing jumps of velocity at collision is to consider a massless interface stuck on the hammer head (this can be seen as a crude representation of the felt around a real hammer head, as shown in figure 2).

Indeed, since the contact occurs between the string and a massless body, $[\![v_s]\!]_{t_c} = 0$. Moreover, since the head of the hammer and the felt are stuck, the points on the common frontier move at the same velocity. Therefore the hammer head cannot be submitted to an impulse force due to collision (the contact point with the string now belongs to the interface, i.e. the felt).

Finally, in the refined model, the wood part of the hammer (including the head and the shank) is described by its modal basis, possibly including viscous damping (here again, in this article, a single mode model is used for simplicity) while the massless interface is described only by its visco-elastic properties. The principle of this model is sketched on figure 3 where u is the compression of the felt, e is the felt thickness at rest, F (resp. $-F$) is the force exerted by the felt on the hammer (resp. on the string), x_s is the position of the contact point on the string, and x_h is the position of the contact point between the hammer and the felt.

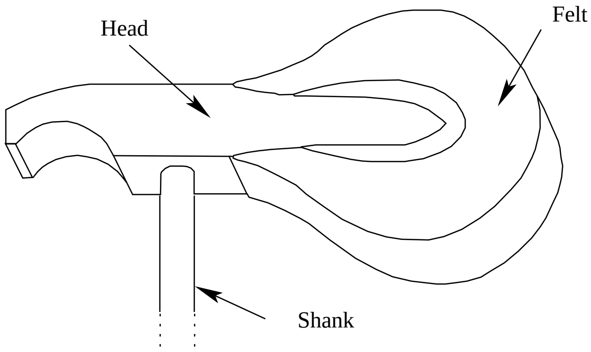

Figure 2: Scheme of a real hammer (drawn according to picture $http://www.ptg.org/images/hmrgood.gif$).

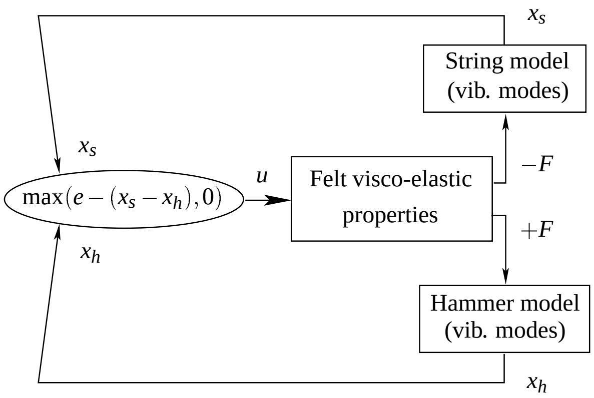

Figure 3: General functionning of the refined hammer/string collision model

III.2. Model Of The Felt Visco-elastic Properties

Among other rather simple models ([9], [10]), the model considered to describe the visco-elastic properties of the felt is the one proposed by Stulov ([4]). According to this model (proposed in relation to hereditary mechanics principles), the felt force response F to a compression u is given by:

$$F(u(t)) = F_0 \left[u^p(t) - \frac{\varepsilon}{\tau} \int_0^t u^p(\xi) e^{\frac{\xi - t}{\tau}} d\xi \right] \quad (6)$$

where F_0 is the felt stiffness constant, p is the stiffness nonlinearity exponent, ε and τ control the history-dependent properties of the material.

This model has been chosen for its good ability to reproduce the measured interaction force when a hammer hits a rigid surface (as shown by Stulov [4] according to measurements by Yanagisawa and Nakamura ([11]), or more recently Stulov in [12] according to its own measurements).

IV. SIMULATION RESULTS

IV.1. Parameters Identification

Parameters F_0, ε, τ and p have been chosen to fit experimental data of Yanagisawa and Nakamura ([11]) given by Suzuki and Nakamura in [6] (fig. 14 p60) and by Stulov in [4] (fig. 2 p2581). These experimental

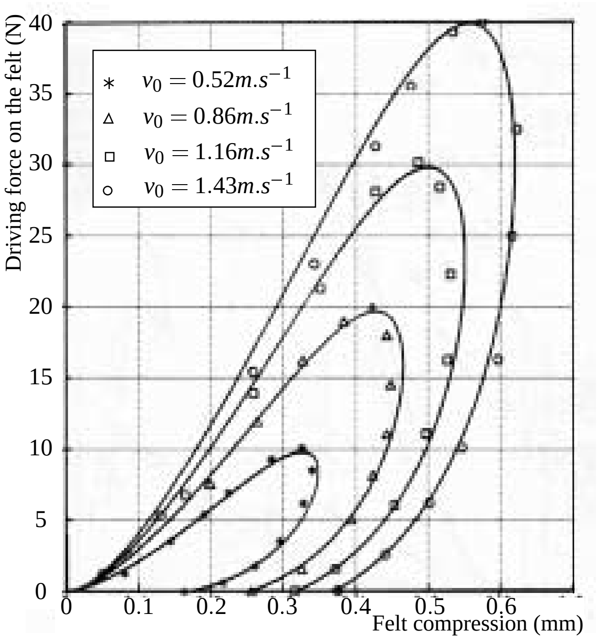

Figure 4: Simulation results (plain lines) and experimental data (symbols) of a $A1$ hammer hiting a rigid surface for different input velocities ($v_0 = 0.52ms^{-1}$, $v_0 = 0.86ms^{-1}$, $v_0 = 1.16ms^{-1}$, $v_0 = 1.43ms^{-1}$). The model used for simulations is described in section III. Experimental data have been obtained by [11] and are taken from [4].

data are force(F)/compression(u) characteristics when a hammer hits a rigid surface for different initial velocities.

For example, for a hammer $A1$ (which mass is $m = 13g$) used for note $A0$, estimated values are $F_0 = 5.77e^6$kN.m^{-p}, $\varepsilon = 0.936$, $\tau = 18e^{-6}$s and $p = 2.2$. This estimation has been done after many simulation trials, as previously done by Stulov in [4] with a simpler hammer model.

IV.2. Rigid (no vibrating) String

The simulation results of a $A1$ hammer hiting a rigid surface are presented in figure 4 for different input velocities ($v_0 = 0.52ms^{-1}$, $v_0 = 0.86ms^{-1}$, $v_0 = 1.16ms^{-1}$, $v_0 = 1.43ms^{-1}$) as plain lines. Parameters of the model are those estimated in section IV.1. The hammer is modeled by a single-mode system. In figure 4 experimental results of Yanagisawa and Nagasaki ([11] given in [4]) are also presented (marqued as symbols) for different initial velocities.

Simulation and experimental results presented in figure 4 are now compared quantitatively in table I, where v_0 is the initial velocity, F_{max} is the maximum value of the driving force on the felt, $u|_{F=F_{max}}$ is the compression of the felt when the maximum driving force F_{max} is reached, $u|_{t=t_r}$ is the compression of the felt at release, u_{max} is the maximum value of the felt compression, and $F|_{u=u_{max}}$ is the driving force on the felt when the maximum value of the felt compression u_{max} is reached.

Simulation results are rather close to experimental

$v_0 = 0.52$ (m.s^{-1})	F_{max} (N)	$u\|_{F=F_{max}}$ (mm)	$u\|_{t=t_r}$ (mm)	u_{max} (mm)	$F\|_{u=u_{max}}$ (N)
Expe.	10	0.323	0.16	0.34	8.35
Simu.	9.76	0.33	0.17	0.34	8.51
$v_0 = 0.86$ (m.s^{-1})	F_{max} (N)	$u\|_{F=F_{max}}$ (mm)	$u\|_{t=t_r}$ (mm)	u_{max} (mm)	$F\|_{u=u_{max}}$ (N)
Expe.	20	0.42	0.26	0.45	14.52
Simu.	19.70	0.43	0.26	0.47	15.93
$v_0 = 1.16$ (m.s^{-1})	F_{max} (N)	$u\|_{F=F_{max}}$ (mm)	$u\|_{t=t_r}$ (mm)	u_{max} (mm)	$F\|_{u=u_{max}}$ (N)
Expe.	30	0.49	0.32	0.53	22.34
Simu.	29.90	0.50	0.32	0.55	23.28
$v_0 = 1.43$ (m.s^{-1})	F_{max} (N)	$u\|_{F=F_{max}}$ (mm)	$u\|_{t=t_r}$ (mm)	u_{max} (mm)	$F\|_{u=u_{max}}$ (N)
Expe.	40	0.57	0.38	0.62	32.63
Simu.	40.12	0.56	0.37	0.62	30.45

TABLE I: Comparison between experimental results obtained by [11] (given in [6] and [4]) and simulation results using the model described in section III.

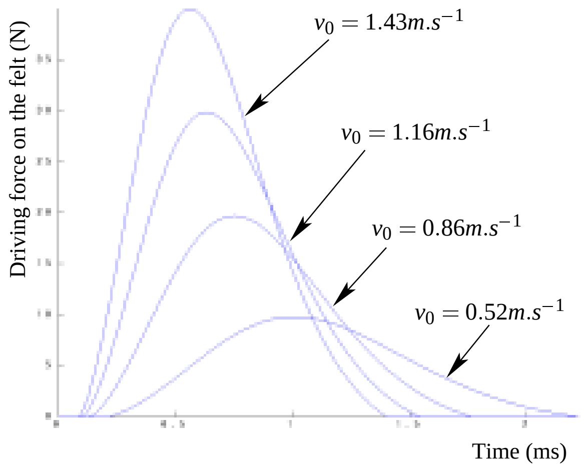

Figure 5: Time domain representation of the simulation results presented in figure 4.

ones, which confirms the conclusion drawn by Stulov for a simpler hammer model (a rigid mass plus the felt). Moreover, it can be observed in figure 4 that the higher the impact velocity v_0, the larger the slope of the curve during the loading. This is in agreement with experimental observations of Yanagisawa and Nakamura. However, the experimental data available have been obtained with a low sampling rate. Therefore, some results presented in table I could be refined with additional experiments.

It is also worth noting that the duration of contact and its reduction as the initial velocity is increased (see figure 5 for simulation results) is comparable to experimental results presented by Suzuki in [6].

IV.3. Vibrating String

The string corresponding to the note $A3$ ($220Hz$) is considered in this section. The mass of the corresponding hammer is $m = 10.6g$, and estimated values for the parameters of the model are $F_0 = 2.24e^{13}\text{kN.m}^{-p}$, $\varepsilon = 0.953$, $\tau = 7e^{-6}$s and $p = 3.3$. Again, these numerical values have been estimated according to experimental data obtained by [11] with a rigid string.

First of all, it can be observed in figure 6, that as expected, the velocity v_s of the struck point on the string is now continuous. Modal data of the string used for the simulation are the same as the one used in figure 1.

Next, numerical simulations of Force(F)/compression(u) characteristic and time evolution of F are presented in figure 7 and 8 for an initial hammer velocity $v_0 = 3ms^{-1}$. Their relevance can hardly be evaluated according to experimental results, for two reasons. The first reason is the lack of data available (in fact to the authors' knowledge, only partial experimental results have been published by [13]). The second reason is that simulation results highly depend on the model of the string. Consequently, a direct comparison between simulation and experiment do not allow to evaluate the collision model only.

Finally, simulation results can be analysed and compared to those obtained in the case of a static string, as it is done below. Compared to figure 4, loops can be observed in the force/compression characteristics on figure 7. These loops correspond to ripples in figure 8. They are due to the division of the string into two sub-strings during contact. In figure 8 for example, the string ($220Hz$) is struck at $5/41$ of its length. The ripples observed have a period of $0.52ms$ and correspond to the oscillation of the shortest sub-string (i.e. the length of which is $5/41$ of the string length). Note that the period of a sub-string fixed at both ends should be $5/41$ of $1/220$, i.e. around $0.55ms$. However here, one end of the sub-string is not fixed: indeed, the limit condition is defined by the felt characteristics and is therefore nonlinear. This explains the difference between the measured period (around $0.52ms$) and the period estimated according to the ratio between the string length and the sub-string length (around $0.55ms$). Note that the oscillation period of the longuest sub-string is less than $4ms$, and is of the order of contact duration.

Moreover it can be observed that the contact duration is of the same order as durations experimentaly measured by Hall ([8]) or Askenfelt and Jansson ([14]). Again, simulations for different initial velocities (not presented here) highlight that the larger the impact velocity, the shortest the duration of contact. Compared to simulations done without the model of the felt, larger durations of contact are observed, which probably contributes to the improvement (which has been perceived) of the realism in the synthesized sound.

V. CONCLUSION

This work was mainly motivated by the analysis of sound synthesis results obtained with *Modalys* software when simulating piano sounds. The ham-

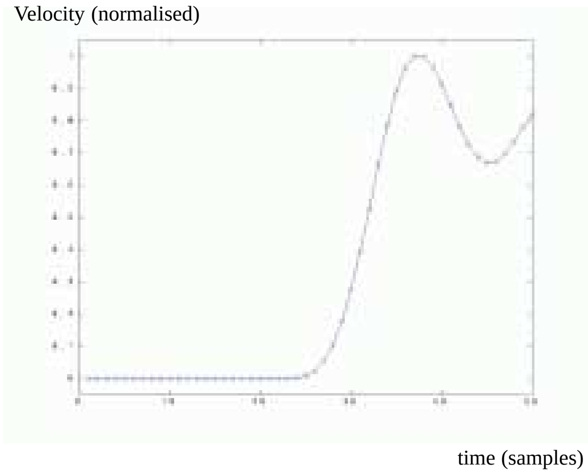

Figure 6: Normalised velocity v_s of the struck point of a string, without any discontinuity at contact time (hammer head covered with felt).

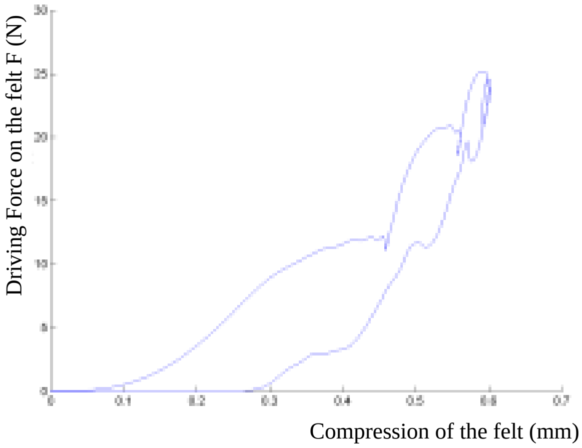

Figure 7: Force(F)/compression(u) characteristic: simulation results of a hammer hiting the A3 string ($220Hz$) at $5/41$ of the string length. Initial velocity is $v_0 = 3ms^{-1}$. The model is described in section III.

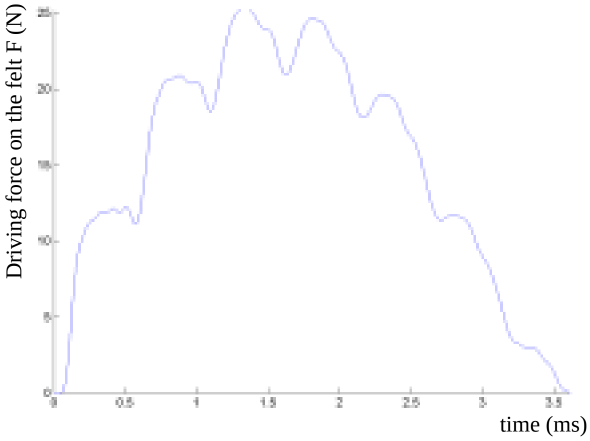

Figure 8: Time domain representation of the simulation results presented in figure 7.

mer/string collision has been considered. After having shown that the Lumped Elastic Collision Model (used in *Modalys*) was responsible for two annoying sound characteristics (a click at contact time, and a resemblance with a plucked string), the model was modified in order to get rid of these artefacts. In practice, the model improvement corresponds to the inclusion of a massless felt around the wood-head of the hammer. Visco-elastic properties of the felts have been modeled using Stulov approach. The modal approach is kept to describe the hammer (i.e. the head, the shank ...) and the string.

From a sound synthesis point of view, the model is promising. Our efforts are now mainly concentrated on two goals. The first goal is to build a real-time software in order to evaluate the model within a live musical context. The second goal consists in carrying out experiments in order to feed the model with the best parameters for each hammer. These parameters should fit experimental data both in the static and in the dynamic cases (which remains an open question). The ability of the Stulov model to reproduce experimental data will then be evaluated more systematically and compared to other recent approaches ([10]).

Acknowledgements: the authors want to thank Joël Bensoam for very profitable discussions and suggestions.

REFERENCES

1. M. Lanza. Erba nera che cresci segno nero tu vivi, 1999.
2. V. Roussarie. *Analyse perceptive de structures vibrantes simulées par modèle physique*. PhD thesis, Université du Maine, Le Mans, 1999.
3. J. M. Adrien and J. Morison. MOSAIC: A Modular Program For Synthesis Using Modal Superposition. In *Modèles Physiques: Création Musicale et Ordinateur*, volume 2, pages 371–384. ACROE, 1990. Current name of MOSAIC is MODALYS.
4. A. Stulov. Hysteretic model of the grand piano hammer felt. *J. Acoust. Soc. Amer.*, 97(4):2577–2585, 1995.
5. G. Weinreich. Coupled piano strings. *J. Acoust. Soc. Amer.*, 62(6):1474–1484, 1977.
6. H. Suzuki and I. Nakamura. Acoustics of pianos. *Applied Acoustics*, 30:147:205, 1990.
7. J. Bensoam. Chocs entre systèmes masses/ressorts. Technical report, Ircam, 2002.
8. D. E. Hall. *Five lectures on the acoustic of the piano*, volume 64, chapter The hammer and the string. Royal Swedish Accademy of Music, 1990.
9. X. Boutillon. Model for piano hammers: Experimental determination and digital simulation. *J. Acoust. Soc. Amer.*, 83(2):746–754, February 1988.
10. F. Avanzini and D. Rochesso. Modelling Collision Sounds: Non-linear Contact Force. In *Proceedings of the COST G6 Conference on Digital Audio Effects*.
11. T. Yanagisawa and K. Nakamura. Trans. Musical Acoust. Techn. Group. In *Meeting Acoust. Soc. Jpn.*, volume 1, pages 14–18, 1982.
12. A. Stulov and A. Mägi. Piano Hammer: Theory and Experiment. In *Proceedings of ISMA'2001*, pages 215–220, 2001.
13. N. Giordano and J. P. Millis. Hysteretic Behavior of Piano Hammers. In *Proceedings of ISMA'2001*, pages 237–240, 2001.
14. A. Askenfelt and E. V. Jansson. From touch to string vibrations.I: Timing in the grand piano action. *J. Acoust. Soc. Amer.*, 88(1):52–63, July 1990.